Supporting Information for

Nanoscopic visualization of restricted non-volume cholinergic and monoaminergic transmission with genetically encoded sensors

Paula K. Zhu[1,2,3,11], W. Sharon Zheng[4,5], Peng Zhang[4], Miao Jing[1,6], Philip M. Borden[7,12], Farhan Ali[8], Kaiming Guo[4,9], Jiesi Feng[1], Jonathan S. Marvin[7], Yali Wang[4], Jinxia Wan[1], Li Gan[10], Alex C. Kwan[8], Li Lin[9], Loren L. Looger[7], Yulong Li[1], Yajun Zhang[1,4,*]

[1]State Key Laboratory of Membrane Biology and Peking-Tsinghua Center for Life Sciences, Peking University, Beijing 100871, China

[2]Math, Engineering & Science Academy Class of 2020, Albemarle High School, Charlottesville, VA 22901

[3]Summer Secondary School Neurobiology Class of 2019, Harvard University, Cambridge, MA 02138

Departments of [4]Pharmacology and [5]Biomedical Engineering Class of 2021, University of Virginia School of Medicine, Charlottesville, VA 22908

[6]Chinese Institute for Brain Research, Beijing 100871, China

[7]Janelia Research Campus, Howard Hughes Medical Institute, Ashburn, VA 20147

[8]Department of Psychiatry, Yale University School of Medicine, New Haven, CT 06511

[9]School of Pharmaceutical Sciences, Wenzhou Medical University, Wenzhou 325035, China

[10]Helen and Robert Appel Alzheimer's Disease Research Institute, Weill Cornell Medicine College, New York, NY 10065

[11]Current address: Undergraduate Class of 2024, Harvard College, Cambridge, MA 02138

[12]Current address: LifeEDIT, Research Triangle Park, NC 27709

METHODS

Animals

Male and female C57BL/6J mice (Jackson Laboratory) were used in this study. Animals were maintained in the animal facility at the University of Virginia and family or pair housed in the temperature-controlled animal room with 12-h/12-h light/dark cycle. Food and water were available *ad libitum*. All procedures for animal surgery and maintenance were performed following protocols approved by the Animal Care & Use Committee of the University of Virginia and in accordance with US National Institutes of Health guidelines.

Acute brain slice preparation

Acute entorhinal cortical, hippocampal, amygdala and midbrain, as well as pancreatic and adrenal tissue slices were prepared from P25-60 animals deeply anesthetized by xylazine-ketamine as described in our previous reports[1-3]. The animals were decapitated and the brain block containing the entorhinal cortex, hippocampus, amygdala or midbrain was quickly removed, and the pancreas or adrenal grand was quickly dissected, before placing into cold (0−4°C) oxygenated physiological solution containing (in mM): 125 NaCl, 2.5 KCl, 1.25 NaH_2PO_4, 25 $NaHCO_3$, 1 $MgCl_2$, 25 D-glucose, and 2 $CaCl_2$, pH 7.4. The brain blocks were directly sectioned into 400-μm-thick brain tissue slices, while the pancreas and adrenal grand were first embedded in low-melting temperature agar (2.5% in PBS) and then sectioned into 400-μm-thick tissue slices, using a DSK microslicer (Ted Pella Inc.). The tissue slices were kept at 37.0 ± 0.5 °C in oxygenated physiological solution for ~0.5−1 hour before imaging. During imaging, the slices were submerged in a chamber and stabilized with a fine nylon net attached to a platinum ring. The recording chamber was perfused with oxygenated physiological solution. The half-time for the bath solution exchange was ~6 s, and the temperature of the bath solution was maintained at 34.0 ± 0.5 °C. All antagonists were bath applied.

Sindbis and lentivirus preparation and expression

Genetically encoded ACh and monoamine fluorescent sensors were sub-cloned into Sindbis and/or lentiviral constructs, and viral particles were produced following our previous studies[2-4]. In brief, fluorescent sensors were sub-cloned into Sindbis viral vector pSinREP5 with the cloning sites Xba1 and Sph1, and into lentiviral vector

pLenti- with the cloning sites BamH1 and Xho1/Not1 under the human Synapsin-1 promoter to ensure neuronal expression or under a GFAP promoter to ensure astrocytic expression.

Expression of genetically encoded fluorescent sensors was made as previously reported[4, 5]. P25−60 animals were initially anesthetized by an intraperitoneal injection of ketamine and xylazine (10 and 2 mg/kg, respectively), and then placed in a stereotaxic frame. A glass pipette was used to penetrate into the entorhinal cortex, amygdala, locus coeruleus, lateral geniculate nucleus and striatum according to stereotaxic coordinates, or the surgically exposed pancreas and adrenal gland, to deliver ~50 nl of Sindbis or lentiviral solution by pressure injection to infect neurons and non-neuronal cells (Sindbis virus) or astrocytes (lentivirus). Experiments were typically performed within 18 ± 4 h after Sindbis viral infection or 1−2 weeks after lentiviral infection for optimal expression[2-4].

Fluorescence imaging

Wide-field epifluorescence imaging was performed using a Hamamatsu ORCA FLASH4.0 camera (Hamamatsu Photonics, Japan), with a pixel array of 2,048 x 2,048. Fluorescent sensor expressing cells in acutely prepared tissue slices excited by a 460-nm ultrahigh-power low-noise LED (Prizmatix, Givat-Shmuel, Israel)[5, 6]. Fluorescence signals were collected with an Olympus 40x water-immersion objective with a numerical aperture of 0.8 or an Olympus 60x water-immersion objective with a numerical aperture of 1.0. Prior to experiments, the imaging system was calibrated, which indicated the pixel resolutions to be ~181 nm/pixel and ~121 nm/pixel for the 40x and 60x objectives, respectively. The frame rate of FLASH4.0 camera was set to 10-50 Hz. To synchronize image capture with electrical stimulation, the camera was set to external trigger mode and triggered by a custom-written IGOR Pro 6 program (WaveMetrics, Lake Oswego, OR)-based software PEPOI[6]. Cholinergic and monoaminergic fibers in tissue slices were stimulated with a bipolar electrode placed ~50−200 μm from imaged cells with single or a train of voltage pulses (400 μs, up to 50 V) to evoke transmitter release. Increasing stimulation intensity and frequency typically enhanced transmitter release and fluorescence responses, and reduced the number of distinguishable individual release sites, yet unsurprisingly, did not affect

diffusion spread constants measured from individual release sites (Fig S2). To better isolate individual release sites, moderate stimulation intensity (i.e., 20-30 V) and frequency (i.e., 2-4 Hz) were routinely used in this study.

Nanoscopic imaging analysis

Evoked ΔF/F responses of genetically encoded fluorescent sensor expressing cells were typically imaged for periods from seconds to minutes. To minimize drifting and fluctuating movements, a stable recording/stimulating and imaging setup was used to carry out all imaging experiments[6]. Image analysis was performed using our custom-written MATLAB-based image processing and analysis program (MIPAP), with algorithms created using MATLAB 2018a with MATLAB's Image Processing Toolbox (Mathworks). Briefly, after correcting photobleaching and auto fluorescence, all images were spatially aligned to the initial reference images using an intensity-based registration function to correct the minimal image drifts and fluctuations. Then, the ΔF/F responses at individual pixels were quantified, rescaled and converted into pseudo-color scales to create heatmap images. The maximal electrically evoked ΔF/F responses at individual pixels over time were subsequently plotted to create 3D spatial profiles for individual transmitter release sites. With these, all transmitters examined displayed many consistent and clear release hotspots at ~120-180 nm/pixel resolution, and pixels with the maximal ΔF/F responses were assumed to be the centers of release (see results). To reduce other sources of noise (e.g., pixelation noise and background noise), super-resolution localization microscopy analysis strategies were employed to average over multiple exposures, multiple releases and/or all directions of transmitter diffusion gradients[7-9]. The averaging also improved the resolution, and thus enabled us to solve spatial diffusion profiles of transmitters at the nanoscale level (1-100 nm), and fluorescence ΔF/F intensity profiles normalized to the peak values fit well with a single exponential decay function. The extracted decay constants were defined as the diffusion spread length constants. Diffusion spread constants were calculated only from fluorescence responses at well-isolated released single sites, to avoid potential fluorescence signal contamination from other release sites. The microscopic point-spread functions on our image setup were measured with 23 nm green GATTA beads (GATTAquant GmbH, Hiltpoltstein, Germany) under both 40x and 60x objectives. To correct for microscopic point-spread function diffraction, deconvolution was made for fluorescence responses imaged under 40x and

60x objectives with their respective point-spread functions using Wiener deconvolution algorithms (and verified with Richardson-Lucy deconvolution algorithms).

Statistical analysis

Statistical results were reported as mean±s.e.m. Animals or cells were randomly assigned into control or experimental groups and investigators were blinded to experiment treatments. Given the negative correlation between the variation and square root of sample number, *n,* the group sample size was typically set to be ~10−25 to optimize the efficiency and power of statistical tests. Statistical significances of the means ($p<0.05$; two sided) were determined using Wilcoxon and Mann-Whitney Rank Sum non-parametric tests for paired and non-paired samples, respectively. The data that support the findings of this study and algorithms developed in this study are available from the corresponding author upon request.

Figure S1

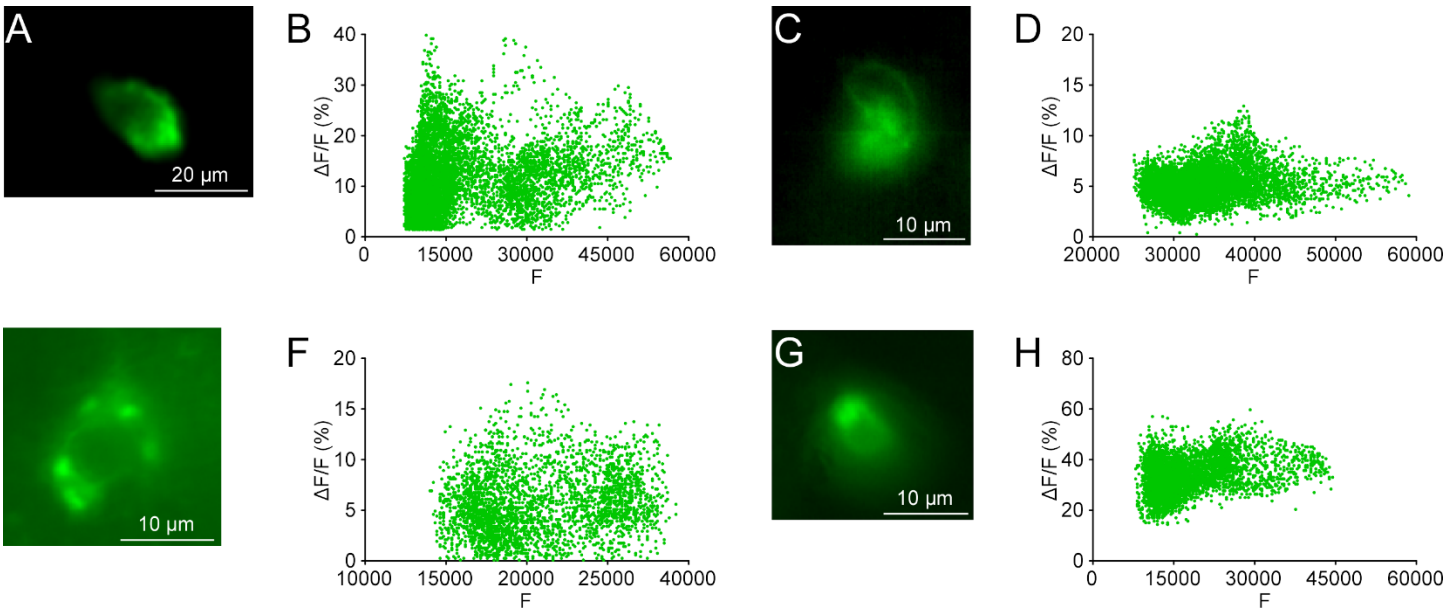

Figure S1. Sensor responses are largely independent of the expression levels.

(**A**) A snapshot of the GACh2.0 expressing MEC stellate neuron shown in Figure **1B**-**D**.

(**B**) Plot of ΔF/F against F of the GACh2.0 expressing neuron shows a weak correlation between ΔF/F and F with a slope value of 0.00000155 (n = 7,219; Normality test $p < 0.001$; Constant variance test $p = 0.151$; r^2 = 0.0571; $F = 436.84$; $p < 0.001$; Linear regression t test).

(**C**) A snapshot of the iAChSnFR expressing MEC stellate neuron shown in Figure **2B**-**D**.

(**D**) Plot of ΔF/F against F of the iAChSnFR expressing neuron shows a weak correlation between ΔF/F and F with a slope value of 0.000000517 (n = 8,515; Normality test $p < 0.001$; Constant variance test $p < 0.001$; r^2 = 0.0348; $F = 307.07$; $p < 0.001$; Linear regression t test).

(**E**) A snapshot of the iAChSnFR expressing MEC stellate neuron shown in Figure **2H**-**I**.

(**F**) Plot of ΔF/F against F of the iAChSnFR expressing neuron shows a weak correlation between ΔF/F and F with a slope value of 0.00000132 (n = 3,038; Normality test $p < 0.001$; Constant variance test $p < 0.001$; r^2 = 0.0251; $F = 78.02$; $p < 0.001$; Linear regression t test).

(**G**) A snapshot of the $GRAB_{NE1m}$ expressing amygdalar neuron shown in Figure **4B**-**D**.

(**H**) Plot of ΔF/F against F of the $GRAB_{NE1m}$ expressing neuron shows a weak correlation between ΔF/F and F with a slope value of 0.00000132 (n = 4,248; Normality test $p = 0.011$; Constant variance test $p < 0.001$; r^2 = 0.135; $F = 637.05$; $p < 0.001$; Linear regression t test). Note no sign of saturation of fluorescence responses

evoked by physiologically released transmitters at these cells, indicating excellent fluorescence response dynamic ranges of GACh2.0, iAChSnFR and $GRAB_{NE1m}$ sensors[5, 10, 11].

Figure S2

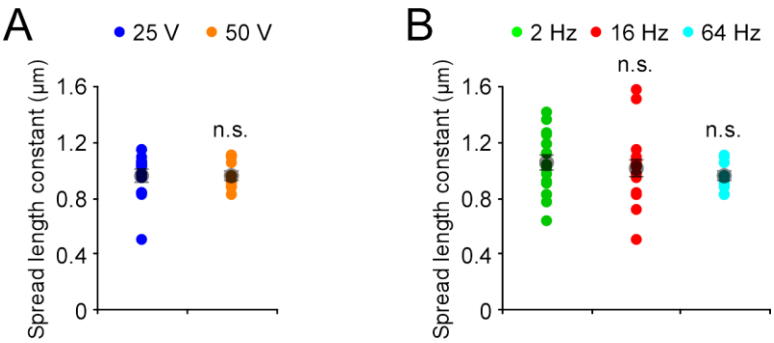

Figure S2. Stimulation intensity and frequency have no effect on diffusion spread length constants.

(**A**) Diffusion spread length constants measured from iAChSnFR expressing neurons stimulated with a train of 25 V or 50 V pulses (25 V: 0.96±0.05 µm, *n* = 13; 50 V: 0.96±0.03 µm, *n* = 9; *U* = 66.0, *p* = 0.640; Mann-Whitney Rank Sum test).

(**B**) Diffusion spread length constants measured from iAChSnFR expressing neurons stimulated with a train of voltage pulses at 16 Hz (1.01±0.06 µm, *n* = 16; *U* = 106.0, *p* = 0.594) and 64 Hz (0.96±0.03 µm, *n* = 9; *U* = 87.0, *p* = 0.257) were comparable to those stimulated at 2 Hz (1.05±0.06 µm, *n* = 15; Mann-Whitney Rank Sum tests). Note values not deconvoluted.

REFERENCES:

1. Wang, G.; Bochorishvili, G.; Chen, Y.; Salvati, K. A.; Zhang, P.; Dubel, S. J.; Perez-Reyes, E.; Snutch, T. P.; Stornetta, R. L.; Deisseroth, K.; Erisir, A.; Todorovic, S. M.; Luo, J. H.; Kapur, J.; Beenhakker, M. P.; Zhu, J. J. $Ca_V3.2$ calcium channels control NMDA receptor-mediated transmission: a new mechanism for absence epilepsy. *Genes & development* **2015,** 29, (14), 1535-51.
2. Zhang, L.; Zhang, P.; Wang, G.; Zhang, H.; Zhang, Y.; Yu, Y.; Zhang, M.; Xiao, J.; Crespo, P.; Hell, J. W.; Lin, L.; Huganir, R. L.; Zhu, J. J. Ras and Rap signal bidirectional synaptic plasticity via distinct subcellular microdomains. *Neuron* **2018,** 98, 783-800.
3. Lim, C. S.; Wen, C.; Sheng, Y.; Wang, G.; Zhou, Z.; Wang, S.; Zhang, H.; Ye, A.; Zhu, J. J. Piconewton-scale analysis of Ras-BRaf signal transduction with single-molecule force spectroscopy. *Small* **2017,** 13, (40), 10.1002/smll.201701972.
4. Lim, C. S.; Kang, X.; Mirabella, V.; Zhang, H.; Bu, Q.; Araki, Y.; Hoang, E. T.; Wang, S.; Shen, Y.; Choi, S.; Kaang, B. K.; Chang, Q.; Pang, Z. P.; Huganir, R. L.; Zhu, J. J. BRaf signaling principles unveiled by large-scale human mutation analysis with a rapid lentivirus-based gene replacement method. *Genes & development* **2017,** 31, (6), 537-552.
5. Jing, M.; Zhang, P.; Wang, G.; Feng, J.; Mesik, L.; Zeng, J.; Jiang, H.; Wang, S.; Looby, J. C.; Guagliardo, N. A.; Langma, L. W.; Lu, J.; Zuo, Y.; Talmage, D. A.; Role, L. W.; Barrett, P. Q.; Zhang, L. I.; Luo, M.; Song, Y.; Zhu, J. J.; Li, Y. A genetically encoded fluorescent acetylcholine indicator for in vitro and in vivo studies. *Nature biotechnology* **2018,** 36, (8), 726-737.
6. Wang, G.; Wyskiel, D. R.; Yang, W.; Wang, Y.; Milbern, L. C.; Lalanne, T.; Jiang, X.; Shen, Y.; Sun, Q.-Q.; Zhu, J. J. An optogenetics- and imaging-assisted simultaneous multiple patch-clamp recordings system for decoding complex neural circuits. *Nature protocols* **2015,** 10, 397-412.
7. Small, A.; Stahlheber, S. Fluorophore localization algorithms for super-resolution microscopy. *Nature methods* **2014,** 11, (3), 267-79.
8. Sauer, M. Localization microscopy coming of age: from concepts to biological impact. *Journal of cell science* **2013,** 126, (Pt 16), 3505-13.
9. Thompson, R. E.; Larson, D. R.; Webb, W. W. Precise nanometer localization analysis for individual fluorescent probes. *Biophys J* **2002,** 82, (5), 2775-83.
10. Borden, P. M.; Zhang, P.; Shivange, A. V.; Marvin, J. S.; Cichon, J.; Dan, C.; Podgorski, K.; Figueiredo, A.; Novak, O.; Tanimoto, M.; Shigetomi, E.; Lobas, M. A.; Kim, H.; Zhu, P. K.; Zhang, Y.; Zheng, W. S.; Fan, C.-C.; Wang, W.; Xiang, B.; Gan, L.; Zhang, G.-X.; Guo, K.; Lin, L.; Cai, Y.; Yee, A. G.; Aggarwal, A.; Ford, C. P.; Rees, D. C.; Dietrich, D.; Khakh, B. S.; Dittman, J. S.; Gan, W.-B.; Koyama, M.; Jayaraman, V.; Cheer, J. F.; Lester, H. A.; Zhu, J. J.; Looger, L. L. A fast genetically encoded fluorescent sensor for faithful in vivo acetylcholine detection in mice, fish, worms and flies. *bioRxiv* **Feb. 8, 2020,** doi: https://doi.org/10.1101/2020.02.07.939504, under review in *Cell*.
11. Feng, J.; Zhang, C.; Lischinsky, J. E.; Jing, M.; Zhou, J.; Wang, H.; Zhang, Y.; Dong, A.; Wu, Z.; Wu, H.; Chen, W.; Zhang, P.; Zou, J.; Hires, S. A.; Zhu, J. J.; Cui, G.; Lin, D.; Du, J.; Li, Y. A genetically encoded fluorescent sensor for rapid and specific in vivo detection of norepinephrine. *Neuron* **2019,** 102, (4), 745-761 e8.

Movie S1. Imaging endogenous acetylcholine release at an entorhinal stellate neuron with GACh2.0

(Please click the start button in **b** to view the video clip)

A 3D spatial and temporal ΔF/F profile

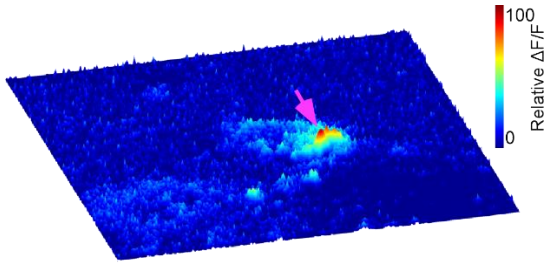

B Electric stimulation-evoked relative ΔF/F

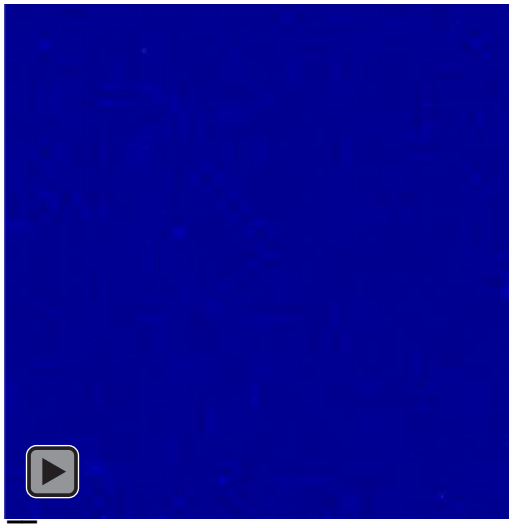

Movie S2. Imaging endogenous acetylcholine release at an entorhinal stellate neuron with iAChSnFR

(Please click the start button in **b** to view the video clip)

A 3D spatial and temporal ΔF/F profile

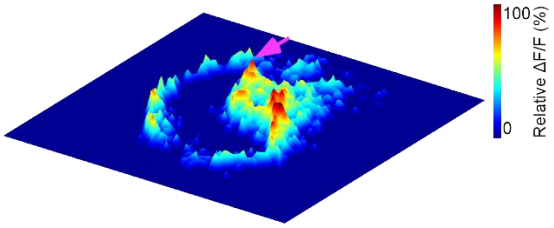

B Electric stimulation-evoked relative ΔF/F

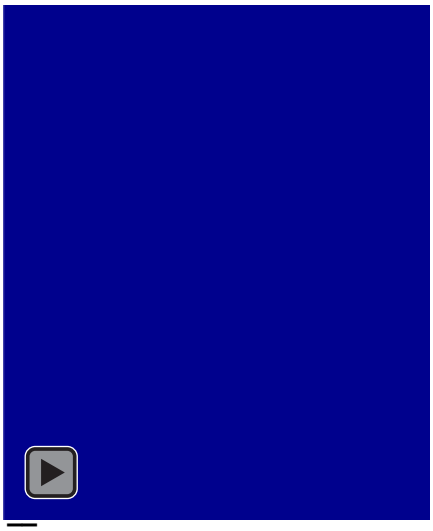

Movie S3. Imaging endogenous acetylcholine release at an entorhinal stellate neuron with iAChSnFR (60x objective)

(Please click the start button in **b** to view the video clip)

A 3D spatial and temporal ΔF/F profile

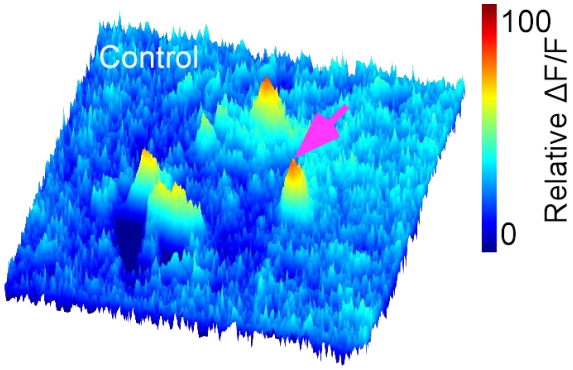

B Electric stimulation-evoked relative ΔF/F

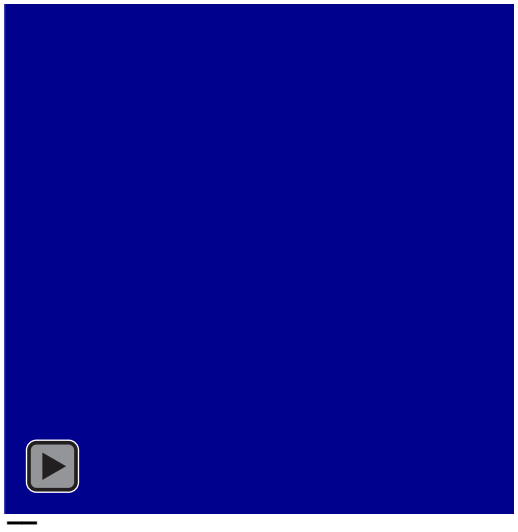

Movie S4. Imaging endogenous norepinephrine release at an amygdalar neuron with GRAB$_{NE1m}$

(Please click the start button in **b** to view the video clip)

A 3D spatial and temporal ΔF/F profile

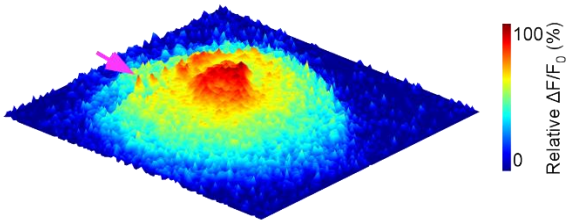

B Electric stimulation-evoked relative ΔF/F